Carbohydrate Polymers 94 (2013) 356–363

Contents lists available at SciVerse ScienceDirect

Carbohydrate Polymers

journal homepage: www.elsevier.com/locate/carbpol

Aluminium and radiation cross-linked carboxymethyl sago pulp beads for colon targeted delivery

Sathasivam Thenapakiam[a], Devakumar Ganesh Kumar[a], Janarthanan Pushpamalar[a], Muniyandy Saravanan[b,*]

[a] School of Science, Monash University, Selangor Darul Ehsan, Malaysia
[b] Jeffrey Cheah School of Medicine and Health Sciences, Monash University, Sunway Campus, 46150 Bandar Sunway, Selangor, Malaysia

ARTICLE INFO

Article history:
Received 17 November 2012
Received in revised form
27 December 2012
Accepted 1 January 2013
Available online 11 January 2013

Keywords:
Carboxymethyl sago pulp
Colon targeted delivery
Ionotropic gelation
Radiation cross-linking
5-Aminosalicylic acid

ABSTRACT

The carboxymethyl sago pulp (CMSP) with a degree of substitution of 0.4% was synthesized from sago waste. The CMSP beads with an average diameter of 3.1–4.8 mm were formed by aluminium chloride gelation as well as further cross-linked by irradiation. To evaluate colon targeted release, a model drug, 5-aminosalicylic acid (5-ASA) was encapsulated in CMSP beads. Fourier-transform infrared spectroscopy and X-ray diffraction studies indicated intact and amorphous nature of entrapped drug. A pH dependent drug release was observed, and about 90% of the drug was released only at pH 7.4 over 9 h. Irradiated beads were resisted the drug release in an acidic environment at a higher extent than non-irradiated beads. The drug release from 6% (w/w) of 5-ASA loaded bead followed zero order, whereas, 15 and 22% loaded beads followed first order. The release exponent *n* value suggests non-Fickian transport of 5-ASA from the beads.

1. Introduction

The conversion of plant waste into useful products has been one of the most important innovations in the recent years. In Sarawak, Malaysia, sago palm (*Metroxylan sagu*) is an important resource of polysaccharides particularly, its starch. Production of the sago starch, however, produced sago waste as its by-product. The synthesis and characterization of carboxymethyl sago pulp (CMSP) hydrogels from sago waste was recently reported by us (Pushpamalar, Langford, Ahmad, Hashim, & Lim, 2013).

Hydrogels are three-dimensional, cross-linked networks of hydrophilic polymers and useful in the formulation of drug-delivery systems. The hydrogels of CMSP was prepared by ionotropic gelation using aluminium chloride as well as irradiation and tested for its efficacy to release the drug in colon. CMSP hydrogels are anionic hydrogels, which have the capacity to swell depending on the pH. The maximum swellings of CMSP irradiated gels at and above pH 7 and low swelling at lower pH are already reported by us. Hence, they are suitable for minimizing the drug release at the gastric pH of 1.2, and to promote the drug release at the colonic pH of 7.4. In the present investigation, the pH sensitive property of CMSP is exploited to deliver the drug in colon.

5-Aminosalicylic acid (5-ASA) is an anti-inflammatory drug used in the treatment of inflammatory bowel disease (IBD) and Crohn's disease (Yang, Chu, & Fix, 2002) was used as a model drug. Administration of 5-ASA in conventional oral drug-delivery systems can lead to serious drawbacks such as pancreatitis, renal toxicity and intestinal nephritis (Schroeder, 2002) as it readily dissolves in the stomach and intestinal fluids, and most of the drug is absorbed before it reaches the colon. Hence, a modified controlled-release dosage form of 5-ASA is required to sustain and target drug effect in colon. As the drug is soluble in acidic and alkaline conditions, it will be useful to study whether the CMSP beads can resist the drug release at acidic conditions or not. The enteric nature of CMSP expected to resist drug release at acidic environment. Though aluminium cross-linked carboxymethyl cellulose material is reported in the literature, production of pH sensitive beads from sago waste is relatively a new area.

In the present investigation, we have incorporated 5-ASA in pH responsive CMSP beads, which can release drug selectively under colonic conditions. 5-ASA loaded CMSP beads were formulated by ionotropic gelation using aluminium chloride and further cross-linked with irradiation in order to restrict the drug release in acidic pH. Drug loaded CMSP beads were then characterized for drug loading, entrapment efficiency, particle size, scanning electron microscopy (SEM), Fourier-transform infrared spectroscopy

* Corresponding author. Tel.: +60 3 55144926; fax: +60 3 55146323.
E-mail addresses: msaravanan72@hotmail.com, drmsaravanan@gmail.com (M. Saravanan).

0144-8617/$ – see front matter © 2013 Elsevier Ltd. All rights reserved.
http://dx.doi.org/10.1016/j.carbpol.2013.01.004

(FT-IR), X-ray diffraction, swelling dynamics and *in vitro* release studies.

2. Materials and methods

2.1. Materials

Sago waste was obtained from PPES Sago Industries (Mukah) Sdn Bhd., Sarawak, 5-aminosalicylic acid (5-ASA) purchased from Lianyungang Zhongyi International Trade Co. Ltd., China. Methanol, isopropanol and ethanol (denatured 95%) obtained from HmbG chemicals, R&M chemicals and Bumi-Pharma Sdn. Bhd., respectively. Sodium chlorite (80% technical grade) was obtained from Sigma–Aldrich and sodium monochloroacetate from Fluka. Aluminium chloride hexahydrate and sodium hydroxide pellets were obtained from Friendemann Schmidt, Malaysia. All other chemicals used were of analytical grade.

2.2. Methods

2.2.1. Preparation of carboxymethyl sago pulp

Carboxymethyl sago pulp (CMSP) was synthesized from sago waste as described in our previous publication (Pushpamalar, Langford, Ahmad, & Lim, 2006). Briefly, 20 g of the Sago waste was transferred into a 1000 ml Erlenmeyer flask and suspended in 640 ml of hot distilled water. 4 ml of glacial acetic acid and 6 g of sodium chlorite were subsequently added. The mixture was later heated to 70 °C for 3 h, then filtered and washed with cold distilled water. The white final residue (sago pulp) was dried in the oven to its constant weight.

5 g of the sago pulp was added into 100 ml of isopropanol and 10 ml of 30% sodium hydroxide. The mixture was stirred for an hour at 160 rpm and 3.0 g of sodium monocholoroacetate was added to the mixture. Then the stirring (160 rpm) was continued at 45 °C for 3 h. The mixture was filtered and suspended in 300 ml methanol overnight and later neutralized with glacial acetic acid. The mixture was filtered again and washed thoroughly with 150 ml of ethanol to remove undesirable products and dried in an oven at 60 °C. The degree of substitution was determined by a titramatic method as explained in our previous publication (Pushpamalar et al., 2006).

2.2.2. Preparation of CMSP beads loaded with 5-ASA

10% (w/v) of CMSP solution was prepared by dissolving synthesized CMSP in 50 ml of distilled water and pH is adjusted to 4 using acetic acid. To this 10, 20 and 30% (w/w) of 5-ASA based on CMSP weight was added and stirred at 800 rpm for 15 min using an automated stirrer. 0.1% (w/w) of sodium metabisulphite was then added to the above mixture according to the amount of 5-ASA (Lachman, Deluca, & Akers, 1987) used. The mixtures were then subjected to sonication with a Hielscher UIP500hd ultrasonic homogenizer at 80% amplitude for 2 min. The beads are produced by dropping polymer–drug mixture using a syringe (10 ml) fitted with 18 number needles into the 5% (w/v) $AlCl_3$ cross-linking solutions containing 0.1% (w/w) sodium metabisulphite. The distance between the needle tip and the top of the $AlCl_3$ solution was fixed at 6 cm. A magnetic stirrer was used to stir the cross-linking solution to keep the beads apart, and the process was carried out in a covered fume hood with no light exposure. Polymer–drug mixtures were introduced in two min duration and then allowed to cure for 15 min with the cross-linking solution. Then, the beads were collected by filtration, washed twice with distilled water and dried at 40 °C for until a constant weight (approx. 24 h) was achieved. The unloaded beads were also prepared in the same manner except without the addition of sodium metabisulphite and 5-ASA.

2.2.3. Determination of irradiation dose for further cross-linking

A 10% (w/v) of CMSP solution was prepared in distilled water. 15 ml samples were then poured separately into rectangular plastic moulds. The moulds were covered with a plastic sheet and subjected to irradiation doses of 5, 10, 15, 20 and 25 kGy using an EPS-3000 electron beam accelerator. All the irradiated samples were transferred into individual tea bags and suspended in beakers containing large amounts of deionised water overnight to obtain the formed hydrogels. The hydrogel residues were then transferred to individual plastic bags and dried in an oven at 70 °C for 3 days. The soluble (% Sol) and gel fractions (% GF) were then calculated as per equations below (Said, Abd Alla, & El-Naggar, 2004), where w_0 and w_1 are the weights of the initial wet hydrogel and the dried hydrogel respectively:

$$\text{Sol fraction}\,(\%) = \left[\frac{(w_0 - w_1)}{w_0}\right] \times 100$$

$$\text{Gel fraction}\,(\text{GF})\,(\%) = 100 - \text{sol fraction}$$

2.2.4. Irradiation of $AlCl_3$ cross-linked CMSP beads

$AlCl_3$ cross-linked beads were prepared as explained in the above procedure and immersed in minimum quantity of normal saline to avoid drying. The beads were stored at 10 °C until irradiated. All beads after reaching room temperature subjected to electron beam (EB) irradiation (10 kGy) to study the combination effects of $AlCl_3$ and irradiation induced cross-linking.

2.2.5. Determination of drug loading and entrapment efficiency

500 mg of drug loaded beads was placed in beakers containing 100 ml of pH 7.4 phosphate buffer and stirred for 24 h at 40 °C with a magnetic stirrer (approx. 200 rpm) to extract the drug. The suspensions were subsequently filtered using filter paper, diluted and the 5-ASA content was measured at 330 nm using a Shimadzu UVmini-1240 UV–vis spectrophotometer. The drug entrapment efficiency (DEE) was then calculated as follows:

$$\text{DEE} = \frac{\text{experimental drug loading}}{\text{theoretical drug loading}} \times 100\%$$

2.2.6. Particle size analysis

The sizes of 100 randomly chosen unloaded and 5-ASA loaded beads were measured at 40× magnification using an Olympus CKX41 projection microscope. The average bead diameter was then calculated using software supplied by the equipment. The photomicrographs were also recorded using the same software.

2.2.7. Scanning electron microscopy (SEM) studies

A Quanta 400 ESEM scanning electron microscope was used to study the shape, size and surface morphology of the beads. Samples were initially coated with a thin layer of gold using a BIO-RAD Polaron division SEM sputter coating system before being observed at 50×, 200× and 30,000× magnifications.

2.2.8. Swelling kinetics

The swelling behaviour of the unloaded and 5-ASA loaded beads were studied by a gravimetric procedure reported by Vázquez, San Roman, Peniche, and Cohen (1997). The study was done in a USP TDT-08L dissolution tester attached with paddle. Respective beads were weighed and added in each vessel containing 600 ml of pH 7.4 phosphate buffer. The swelling rates were measured at 37.0 ± 0.5 °C and 100 rpm. The beads were removed at 30 min intervals over a 5.5–9.5 h period using a plastic sieve and blotted carefully with minimum pressure to remove any excess surface liquid. The swollen beads were then weighed using an electronic

balance. The swelling ratio of the respective beads was determined using the following equation:

$$\text{Swelling ratio (SR)} = \frac{w_t}{w_0}$$

where, w_0 is the initial weight of the dry bead and w_t is the weight of the swollen bead at time t. The equilibrium swelling ratio (ESR) of the respective beads was also determined, where ESR refers to the maximum swelling ratio (SR) of the beads.

2.2.9. Infrared spectroscopy studies

Approximately 0.2 mg of unloaded and 5-ASA loaded beads was separately ground using a mortar and pestle and their infrared spectra measured between 400 and 4000 cm^{-1} using a Varian 640-IR FTIR spectrophotometer using attenuated total reflection (ATR) accessory.

2.2.10. X-ray diffraction

An Olympus InXitu BTXII X-ray diffraction apparatus was used to obtain the X-ray diffraction patterns of the unloaded and drug loaded beads. Each sample was ground to less than 75 μm and homogeneously mixed. Approximately 15 mg of each respective sample was then loaded into the apparatus *via* the sample spinner assembly and a 25 min acquisition produced the diffractograms over a 2θ range. The analysis was performed with a cobalt target X-ray tube operating at 30 kV and 330 μA.

2.2.11. In vitro release studies

The *in vitro* release studies were carried out in a USP dissolution tester (TDT-08L) by paddle method and using 900 ml of 0.1 N HCl (pH 1.2) as the release medium. The amount of beads equivalent to 100 mg of 5-ASA was added to each vessel, and the dissolution rates were measured at 37.0 ± 0.5 °C and 100 rpm. 5 ml of samples was withdrawn at regular intervals, and the same volume of the release medium was replaced. After filtration, the amount of drug present in the sample was estimated at 302 nm using UV–vis spectrophotometer. To simulate colonic conditions the release studies were also carried out at pH 7.4 using phosphate buffers and drug content was measured at 330 nm (Karewicz, Łęgowik, & Nowakowska, 2011) following suitable dilutions.

3. Results and discussion

3.1. Preparation of 5-ASA loaded CMSP beads

The degree of substitution of the CMSP was determined as 0.4. The CMSP solution of 10% (w/v) was chosen as it formed more spherical and consistent size beads. Beads prepared with 2.5, 5 and 7.5% (w/v) CMSP showed high tendency of clumping as well as irregular shapes and sizes. The less viscous nature of these mixtures does not allow much control during extrusion through the needle, thus leading to beads of high variability in shape and size. Moreover, these beads were weak and easily cracked during handling. The beads formed using 12.5% CMSP was large tear-drop shaped due to more viscous nature of polymeric drug mixture, which is difficult to extrude through the needle and might not produce reproducible release kinetics (Mahato & Narang, 2012). Therefore, the 10% CMSP solutions were used to prepare 5-ASA loaded beads. However, higher drug loading resulted in relatively non-spherical beads even with 10% CMSP. The stability of 5-ASA depends on the pH, and it decreases with increasing pH (Palsmeier, Radzik, & Lunte, 1992). The pH of the CMSP solution was above 10, and it would cause 5-ASA degradation. Hence, the pH of the CMSP solution was adjusted to 4 using 0.1% acetic acid before making the final volume adjustment. Later, the drug was added to CMSP solution at pH 4 to minimize drug degradation. A minimum concentration of $AlCl_3$ was determined as 5% (w/v) and below this drug loaded beads did not form well. Based on literature review higher concentration of $AlCl_3$ was avoided to limit aluminium concentration as well as to avoid formation of more rigid beads. Higher gelation may also result in loss of loaded drug due to expulsion by shrunk polymeric network and, which was as well observed in our drug loading study. Instead, irradiation of wet beads was attempted to increase cross-linking without drug loss.

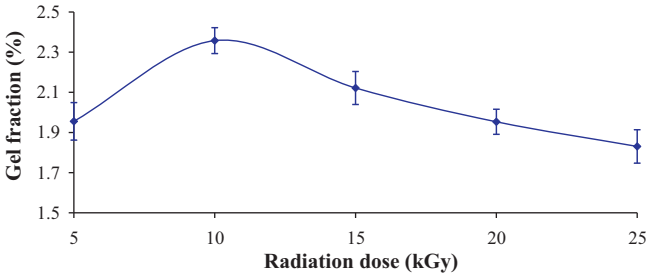

Fig. 1. Influence of irradiation dose on gel fraction of CMSP with a degree of substitution of 0.4. Each data represents average of three determinations ($n = 3 \pm$ sd).

3.2. Influence of irradiation on gel fraction of CMSP

Based on above observations, a 10% (w/v) solution of CMSP was selected and exposed to various radiation doses in order to select appropriate radiation dose for cross-linking. % GF in CMSP increased with increasing radiation dose up to 10 kGy, indicating cross-linking predominates over scission and thus gel formation proportional to radiation dose (Pushpamalar et al., 2013; Vijayabaskar, Bhattacharya, Tikku, & Bhowmick, 2004). At 5 kGy, lower % GF obtained is due to less cross-linking occurring as a result of the lower radiation energy used. As shown in Fig. 1, a drop in % GF are observed with increasing radiation doses beyond 10 kGy, with the moderately viscous solution becoming increasingly more dilute and watery. This reduction in % GF is due to comparatively more scission and oxidative degradation taking place as compared to cross-linking (Pushpamalar et al., 2013). Irradiation of 10% (w/v) CMSP solution using 10 kGy resulted in highest % GF and hence used to further crosslink CMSP beads.

3.3. Drug loading and entrapment efficiency

5-ASA is a water-soluble drug and undergoes oxidative degradation during the loading process. Sodium metabisulphite is added to the polymer drug mixture as well as the cross-linking solution to avoid drug loss during the encapsulation process. As shown in Table 1, 6, 15 and 22% (w/w) 5-ASA loaded beads showed an entrapment efficiency of 68, 88, and 94%, respectively. The loss of the drug could be at the initial stage of cross-linking where the drug is very permeable, and hence there is no control over the loss from the beads. The extent of cross-linking is more at high polymer content as in the case of batch 1 (Table 1), where higher cross-linking expels the drug molecules due to tight arrangement of polymeric network. This could be reasoned for poor encapsulation at lower drug loading. As drug loading increases, the intensity of cross-linking reduces and thus produced better encapsulation. The drug content of the beads after irradiation remains almost same, and it is an evidence that irradiation did not cause drug loss during the cross-linking process.

High water solubility of the encapsulating drug is one of the limiting factors in getting higher encapsulation. However, the solubility of 5-ASA kept to a minimum by adjusting the pH of polymer–drug mixture to the isoelectric point (pH 4) of the drug. The pH of cross-linking solution is also adjusted to 4.3 (Allen,

Table 1
Physicochemical parameters of 5-ASA loaded CMSP beads.

Batch no	Preparation of beads quality used			Actual drug loading (%, w/w)		DEE (%)	Average bead diameter* (mm)		Correlation coefficient (r^2)				Rate constant k				Korsmeyer–Peppas			
	CMSP (g)	Drug (g)	Theoretical drug loading (%, w/w)						Zero order		First order		Zero order (% h^{-1})		First order (h^{-1})		Correlation coefficient (r^2)		*n* value	
				AI[a]	EB[b]		AI[a]	EB[b]	AI[a]	EB[b]	AI[a]	EB[b]	AI[a]	EB[b]	AI[a]	EB[b]	AI[a]	EB[b]	AI[a]	EB[b]
1	5	0.5	9.1	6.16 ± 0.04	6.19 ± 0.08	68	3.82 ± 0.09	3.7 ± 0.08	0.99	0.99	0.96	0.94	10.6	10.2	0.27	0.26	0.99	0.98	0.67	0.66
2	5	1	16.7	14.61 ± 0.09	14.70 ± 0.12	88	4.3 ± 0.08	4.08 ± 0.08	0.92	0.93	0.98	0.99	11.8	10.5	0.33	0.29	0.98	0.99	0.57	0.60
3	5	1.5	23.1	21.66 ± 0.21	21.89 ± 0.33	94	4.78 ± 0.09	4.53 ± 0.08	0.93	0.91	0.99	0.99	12.3	11.1	0.45	0.4	0.99	1	0.60	0.66

* Diameter of unloaded AI[a] and EB[b] beads were 3.35 ± 0.06 and 3.14 ± 0.05, respectively.
[a] Beads prepared with ionotropic gelation alone.
[b] Beads prepared with ionotropic gelation as well as electron beam irradiation.

Weinberger, & Weinberger, 2004) at which the drug is least soluble. This could be the reason for the high DEE observed for all the 5-ASA loaded beads. Hydrogen bonding between the amine groups ($-NH_2$) of 5-ASA and the carboxylate groups ($-COO^-$) of CMSP may also contribute to the high DEE (Li et al., 2006).

3.4. Particle size analysis

As indicated in Table 1, the unloaded were smaller than the drug loaded beads. The average size and size deviation increased with increasing 5-ASA loading. It could be due to an increase in viscosity because of higher drug concentration in the polymeric mixture. Higher drug loadings could distort the bead shape, possibly due to disruption of the matrix by the drug molecules during bead formation and also by exhibiting more resistance when extruding through the needle (Prüsse et al., 2008). As shown in Table 1, all the irradiated beads were smaller than their respective non-irradiated counterparts. This is due to radiation induced further cross-linking leading to a more compact matrix. Typical photomicrographs of beads during the size measurement were illustrated in Fig. 2. An increase in size at higher loading is also evidenced by the photomicrographs.

3.5. Scanning electron microscopy (SEM) studies

The unloaded beads were most spherical in shape and the shape becoming decreasingly spherical and almost oval with increasing 5-ASA loading as evidenced by Fig. 3. As loading increases, an increase in bead size also observed. All irradiated beads were smaller than their respective non-irradiated $AlCl_3$ cross-linked counterparts. These observations were further supporting particle size analysis data obtained by microscopy. As seen in Fig. 1, the surface of the beads tends to get rougher as 5-ASA loading increases. Beads with low drug content might have undergone more extensive cross-linking due to a higher polymer to drug ratio and hence having a smoother surface. Similar observation is also reported by Kangwansupamonkon, Damronglerd, and Kiatkamjornwong (2002) for styrene based beads. As seen in SEM photographs (Fig. 3), the surfaces of the irradiated bead are evener as compared to non-irradiated due to a greater extent of cross-linking between the polymer chains.

3.6. Swelling behaviour

The swelling behaviour of the CMSP beads (Fig. 4) dependent on polymer content and extent of cross-linking in the beads. The equilibrium swelling ratio of (ESR) 5-ASA loaded beads increased with an increasing polymer content. 6% (w/w) drug loaded beads having the greatest ESR, followed by the 15 and then the 22% (w/w) 5-ASA loaded beads. A similar observation is also reported by Boppana, Kulkarni, Setty, and Kalyane (2010) and is due to the increased proportion of the hydrophilic CMSP polymer per unit weight of the bead. This increases the affinity of the lower drug-loaded beads for water, thus giving rise to a greater ESR. It is also observed that the ESRs of all irradiated beads were below their respective non-irradiated $AlCl_3$ cross-linked beads, indicating a comparatively lower extent of swelling. Irradiation might have produced a more rigid hydrogel matrix which could be the reason for reduced water uptake and swelling.

The ESRs of the unloaded beads (Fig. 4) were unexpectedly below that of the 6% (w/w) 5-ASA loaded beads, although they were expected to have higher ESRs due to their greater hydrophilic polymer content (Boppana et al., 2010). This could be due to the higher CMSP content resulting in the highest degree of cross-linking in an extent that both the diffusion of solvent molecules and relaxation of polymer chains are reduced (Graiver, Hyon, & Ikada, 1995). This

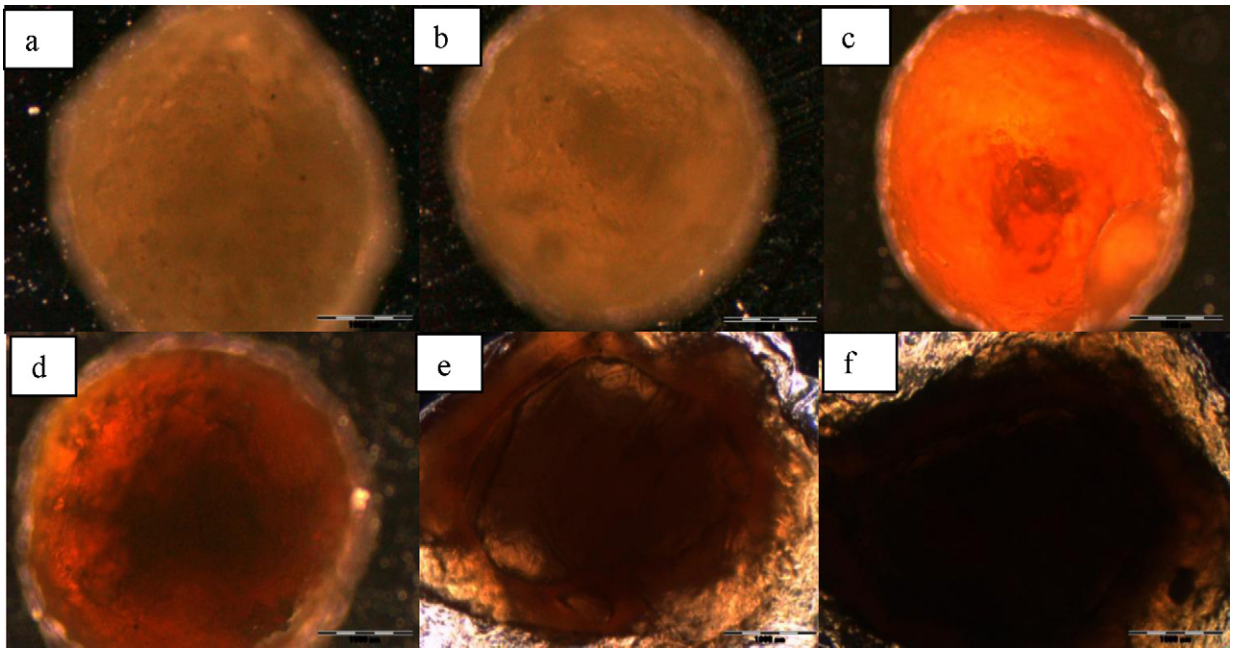

Fig. 2. Photomicrograph of ionotropically crosslinked CMSP beads during particle size measurement. Pictures shows unloaded (a and b), 6% (c and d) and 22% (e and f) (w/w) drug loaded beads. It also indicates apperance of $AlCl_3$ cross-linked beads before (a, c and e) and (b, d and f) after irradiation. The scale shown in the figure equals to 1000 μm.

inflexibility of the hydrogel network causes swelling that becomes independent of the polymer concentration and leads to a lower ESR for the unloaded beads than for the 6% (w/w) 5-ASA loaded beads.

3.7. Infrared spectroscopy studies

The FT-IR of 5-ASA (Fig. 5A) has a characteristic broad band at 2200–3400 cm^{-1} corresponding to the mutual overlapping of —NH and —OH stretching. The peak at 1648 cm^{-1} indicates C=O stretching, a band at 1619 cm^{-1} reveals aromatic C=C stretching and —NH bending. The peaks corresponding to C—C stretching and —COOH stretching were also observed at 1487 cm^{-1} and 1316 cm^{-1}, respectively. Characteristic bands at 1378 cm^{-1} and 1353 cm^{-1} attributed to —OH bending and C—N stretching in 5-ASA, respectively. The similar peaks of 5-ASA were also reported in the literature (Kawadkar, Chauhan, & Ram, 2010; Viseras, Aguzzi, Cerezo, Cultrone, & Viseras, 2009).

The IR spectrum of CMSP showed a broad peak at 3326 cm^{-1} due to stretching vibration of —OH group (Fig. 5B). The peak at 2897 cm^{-1} is due to C—H stretching vibration. The presence of a strong absorption band at 1598 cm^{-1} confirms the presence of $—COO^-$ group and act as evidence of carboxylation of sago pulp. The bands at 1417 and 1319 cm^{-1} are for CH_2 scissors and OH bending vibration, respectively. The broad bands from 1000 to 1200 cm^{-1} were due to sugar ring absorption (Barbucci, Magnani, & Consumi, 2000; Wang et al., 2007).

Fig. 5C shows FT-IR spectrum of $AlCl_3$ cross-linked unloaded CMSP beads. A shift in peak number and intensity observed upon cross-linking which are due to the physicochemical changes occurring upon formation of the CMSP beads. A drop in intensity is observed in the peak at 1598 cm^{-1} due to carboxylate groups (COO^-) upon cross-linking with $AlCl_3$ (Barbucci et al., 2000). This was expected as Al^{3+} form cross-links between CMSP chains *via* these COO^- groups (Boppana et al., 2010; Hosny & Al-Helw, 1998), hence leading to this drop in intensity. A new peak is seen at 1450 cm^{-1} and is due to —CH stretching of cross-links. A new peak also emerges at 1722 cm^{-1} upon cross-linking, which is representative of the —C=O vibration of the protonated carboxylic acid groups involved in hydrogen bonding (Barbucci et al., 2000). This protonation could be from the H^+ present in the $AlCl_3$ aqueous solution. The peak at 3367 cm^{-1} increases upon cross-linking probably due to the increase in inter-molecular hydrogen bonding of the polymer chains due to their closer proximity. The irradiated beads also showed similar bands (Fig. 5D) as that of non-irradiated.

As shown in Fig. 5E and F, a slight shift in some peaks of both CMSP and 5-ASA in the spectra of 15% (w/w) beads were noticed. However, most of the characteristic peaks of 5-ASA were appeared in the drug loaded beads and revealed no polymer drug interaction. Moreover, no changes in drug peaks were observed after irradiation (Fig. 5F) and indicate stable nature of drug at the applied radiation dose. Similar observations were also seen in 6 and 22% (w/w) loaded beads and support the data obtained in the drug loading analysis.

3.8. X-ray diffraction

The X-ray diffraction of 5-ASA is shown in Fig. 6A, the crystalline nature of the drug confirmed by various crystalline peaks observed at different degrees. No prominent peaks (Fig. 6B) were observed in unloaded CMSP beads indicating amorphous nature of CMSP in the formulated beads. The X-ray diffraction pattern of 6% (Fig. 6C), 15% (Fig. 6D) and 22% (Fig. 6E) (w/w) drug loaded beads were almost similar to that of the unloaded beads. However, 22% (w/w) loaded bead has shown less intensive crystalline drug peaks in the range of 15–20 and 25–35 degrees suggesting the presence of crystalline form. As the peaks are less intensive, the drug might have presented as a mixture of amorphous and crystalline form. The beads with 6 and 15% (w/w) drug loading has shown no prominent crystalline drug peaks and indicated complete amorphous nature of the entrapped drug.

3.9. In vitro drug release studies

As shown in Fig. 7A and B, more sustained drug release observed in the 6% loaded beads followed by 15 and 22% loaded beads. In spite of lower size and high surface area, 10% loaded beads produced more sustained release. This is due to higher polymer to drug ratio that causes an increase in cross-linking with greater

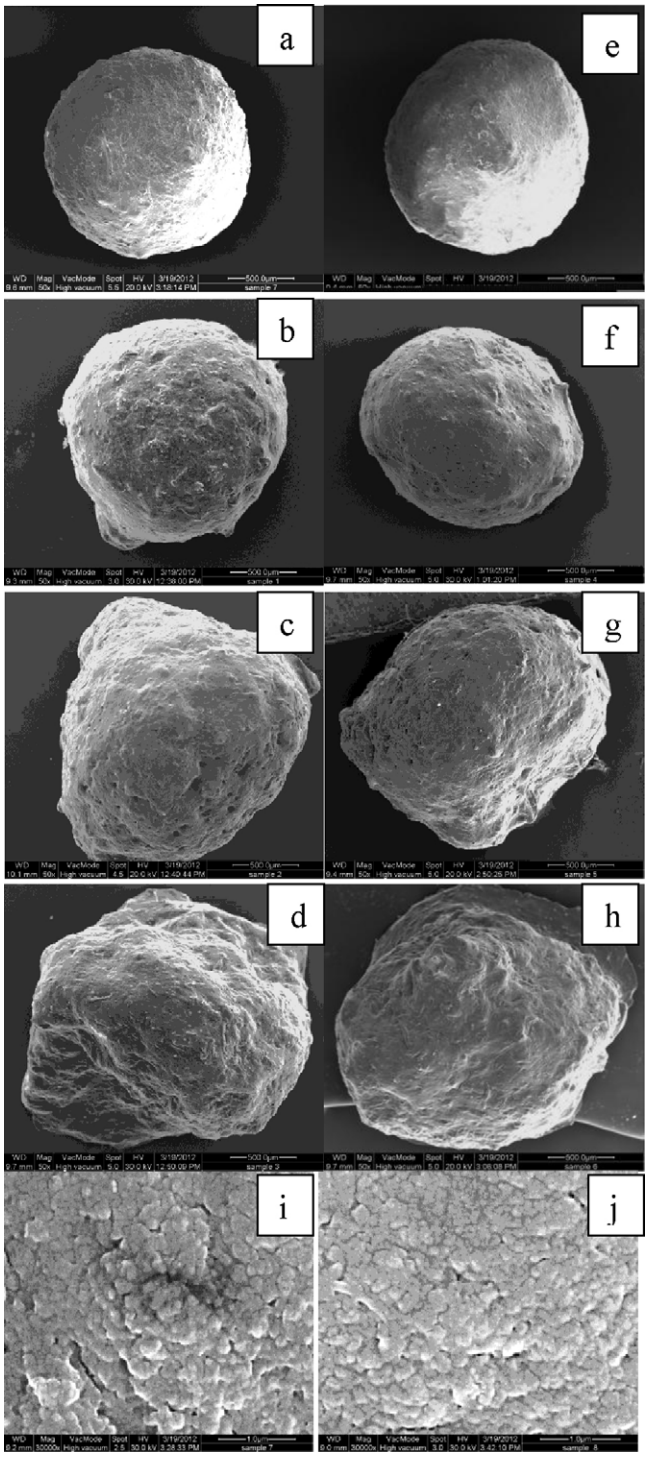

Fig. 3. SEM pictures of $AlCl_3$ cross-linked CMSP beads before (a, b, c, d and i) and after irradiation (e, f, g, h and j). The figure also shows the unloaded (a and e), 6% (b and f), 15% (c and g) and 22% (d and h) (w/w) 5-ASA loaded beads. The picture also shows surface morphology of beads before (i) and after irradiation (j).

rigidity, and less water permeability resulted in slower drug release. All irradiated beads have slightly more sustained release as compared to their respective non-irradiated beads. This confirms that the irradiation could further sustain the drug release in ionotropically cross-linked CMC microspheres. An initial burst release was observed, and it could be due to the presence of drug at the surface of the beads as well as from loosely bound drug. The burst release was proportionally increased with higher drug loading.

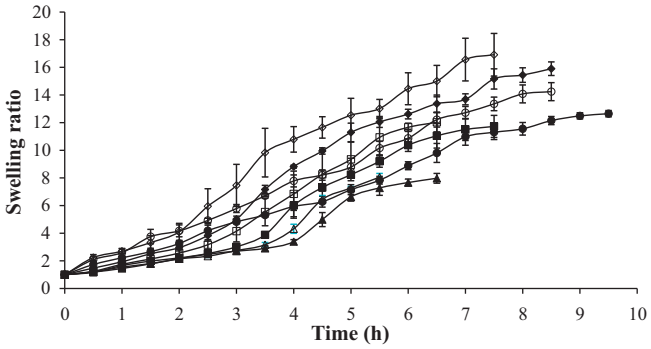

Fig. 4. Dynamic swelling profile of unloaded (○ and ●), 6% (◊ and ♦), 15% (□ and ■) and 22% (Δ and ▲) (w/w) 5-ASA loaded CMSP beads cross linked by $AlCl_3$ (open symbols) as well as irradiation (closed symbols), $n = 3 \pm$ sd.

As shown in Fig. 7A, the maximum release of 5-ASA at pH 1.2 was less than 6% even after 4 h. It was less than a reported 8.4–11.9% release from alginate beads (Tuğcu-Demiröz, Acartürk, Takka, & Konuş-Boyunağa, 2007). In an acidic medium, the anionic COO^- groups in CMSP are protonated and hence the main anion-anion repulsion forces are eliminated (Pourjavadi, Jahromi, Seidi, & Salimi, 2010) which might have produced unswollen state of beads and prevented the drug release. The p*K*a value of CMSP is between 3.8 and 4.2, at pH below the p*K*a value the polymeric material will be in unionized form and thus less or no interaction with dissolution medium due to hydrophobic nature. At pH above the p*K*a value, the polymeric bead become ionizable and hydrophilic hence releases the drug.

As seen in Fig. 7B, all formulated beads could release the drug in the phosphate buffer at pH 7.4 in a sustained manner over 6–9 h. At pH 7.4, CMSP beads begin to swell due to the development of osmotic swelling forces (Pushpamalar et al., 2013). This phenomenon arises as a result of their unprotonated COO^- groups,

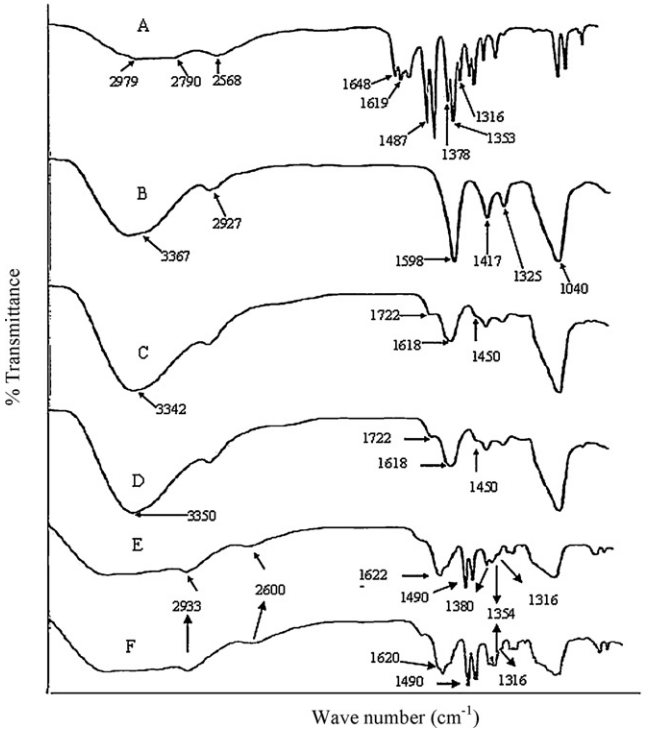

Fig. 5. FTIR spectra of 5-ASA (A), CMSP (B), unloaded CMSP beads cross-linked by $AlCl_3$ before (C) and after irradiation (D), 15% (w/w) 5-ASA loaded CMSP beads cross-linked by $AlCl_3$ before (E) and after irradiation (F).

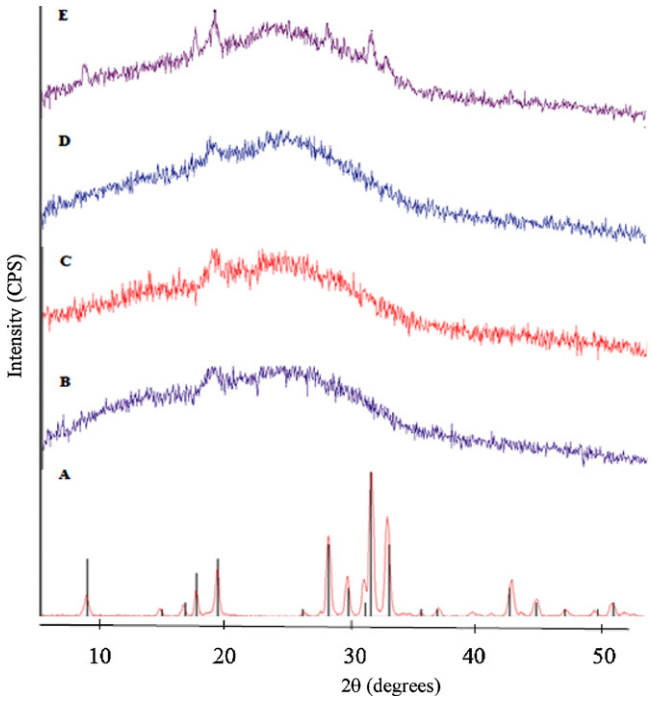

Fig. 6. X-ray diffraction of 5-ASA (A), unloaded (B), 6% (C), 15% (D) and 22% (E) (w/w) 5-ASA loaded CMSP beads cross-linked by $AlCl_3$ as well as irradiation.

which are completely ionized at this pH. The higher solubility of the 5-ASA drug at pH 7.4 might also contribute to a faster drug release. As indicated in the swelling studies (Fig. 4), all the beads, had reached their ESRs 30 min before the end of their respective drug release profiles. This could be due to reaching the maximum swelling, and any remaining drug from the bead cores would have been released in the dissolution medium by that time.

3.10. Release kinetics

Data obtained from *in vitro* release studies (pH 7.4) were fitted to (Saravanan, Bhaskar, Maharajan, & Pillai, 2004) zero and first order equation. The following plots were made: Q_t vs. t (zero order kinetic model), and log $(Q_0 - Q_t)$ vs. t (first order kinetic model). Where, Q_t is the amount of drugs released at time t and Q_0 is the initial amount of the drug present in the microspheres. Further, to confirm the mechanism of drug release, first 60% drug release was fitted in Korsmeyer–Peppas model

$$\frac{M_t}{M_\alpha} = kt^n$$

where M_t/M_α is the fraction of drug released at time t, k is the rate constant and n is the release exponent. The n value is used to characterize different release mechanisms.

As shown in Table 1, the order of drug release depended on the drug loading. Lower drug loaded beads followed zero order and higher drug loading resulted in first order release. 6% (w/w) loaded beads shown a zero order of release as the data were almost fit in to zero ($r^2 > 0.99$) than the first order ($r^2 < 0.96$). However, beads with 15 and 22% (w/w) loaded beads have shown higher correlation with first order ($r^2 > 0.98$) than zero order ($r^2 < 0.93$). This could be due to presence of surface or loosely bound drug in the beads with higher drug loading. The loosely bound or surface drug produced an initial high release due to burst effect and thus showed a first order release kinetics. In contrast, at low drug loading drugs were well encapsulated and the release was slow and steady due diffusion and swelling mechanism. Higher correlations ($r^2 > 0.98$) were

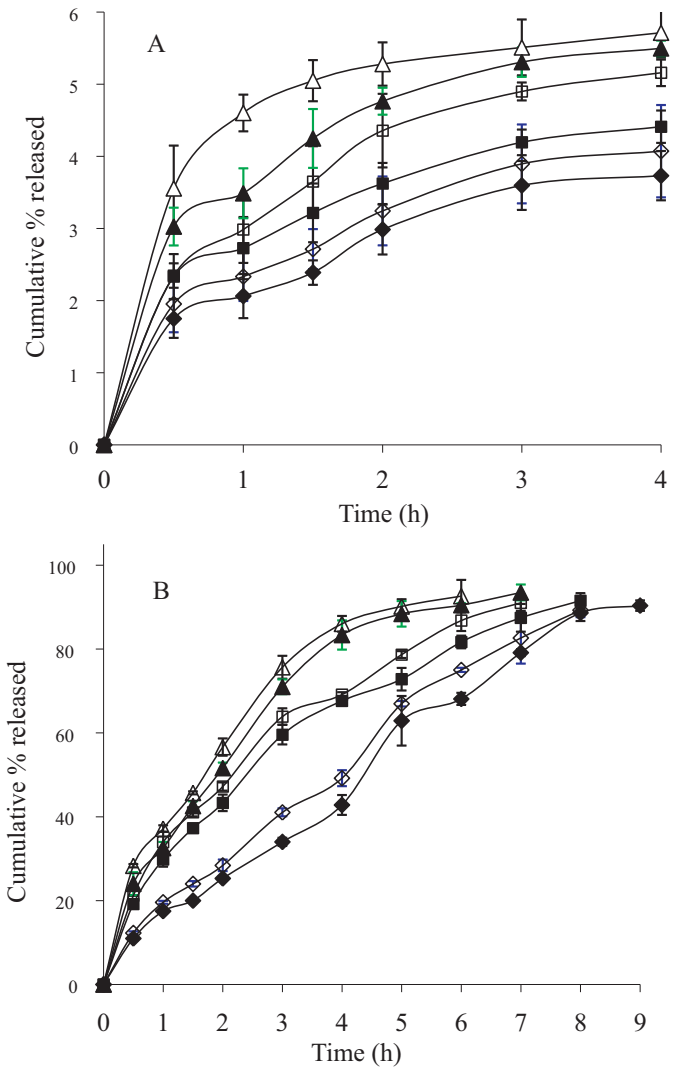

Fig. 7. *In vitro* release profile of 5-ASA from 6% (◊ and ♦), 15% (□ and ■) and 22% (Δ and ▲) (w/w) loaded CMSP beads in pH 1.2 (A) and pH 7.4 (B) ($n = 3 \pm$ sd). Open and closed symbols represent beads cross linked by $AlCl_3$ alone and with irradiation, respectively.

obtained in Korsmeyer–Peppas equation for all types of drug loading. The value of the exponent n was found between 0.57 and 0.67 indicating non-Fickian or anomalous release mechanism (Ritger & Peppas, 1987).

The radiation cross-linking caused significant changes in the rate constant and n value at higher drug loading (15 and 22%, w/w). The rate constants of these irradiated beads (Table 1) were lesser than the non-irradiated counterpart and indicating slower drug release. The higher n value was also observed in high drug loaded irradiated beads. In contrast, irradiation produced little or no changes in these parameters with 6% (w/w) loaded beads.

4. Conclusions

The present investigation clearly indicated the possibility of developing colon targeted drug delivery system using 0.4 substituted CMSP obtained from Malaysian sago waste. Ionic, as well as radiation cross liking, could be used to optimize the drug release profile. The drug release was low and negligible at the stomach pH, and a sustained drug release observed in the colonic pH. Since the product is developed from industrial waste, it would be useful in reducing pollution, as well as the cost of the formulation.

Declaration of interest

The author reports no conflicts of interest. The author alone is responsible for the content and writing of the paper.

Acknowledgement

The authors would like to acknowledge Malaysian Nuclear Agency, Malaysia for their help in the EB irradiation.

References

Allen, L., Weinberger, J., & Weinberger, R. (2004). Determination of impurities in the drug 5-aminosalicylic acid by micellar electrokinetic capillary chromatography using an electrolyte pH that approaches the isoelectric point of the parent compound. *Journal of Chromatography A*, *1053*(1), 217–226.

Barbucci, R., Magnani, A., & Consumi, M. (2000). Swelling behavior of carboxymethylcellulose hydrogels in relation to cross-linking, pH, and charge density. *Macromolecules*, *33*(20), 7475–7480.

Boppana, R., Kulkarni, R. V., Setty, C. M., & Kalyane, N. V. (2010). Carboxymethylcellulose-aluminium hydrogel microbeads for prolonged release of simvastatin. *Acta Pharmaceutica Sciencia*, *52*, 137–143.

Graiver, D., Hyon, S. H., & Ikada, Y. (1995). Poly(vinyl alcohol)–poly(sodium acrylate) composite hydrogels. I. Kinetics of swelling and dehydration. *Journal of Applied Polymer Science*, *57*(11), 1299–1310.

Hosny, E. A., & Al-Helw, A. A. R. M. (1998). Effect of coating of aluminum carboxymethylcellulose beads on the release and bioavailability of diclofenac sodium. *Pharmaceutica Acta Helvetiae*, *72*(5), 255–261.

Kangwansupamonkon, W., Damronglerd, S., & Kiatkamjornwong, S. (2002). Effects of the crosslinking agent and diluents on bead properties of styrene–divinylbenzene copolymers. *Journal of Applied Polymer Science*, *85*(3), 654–669.

Karewicz, A., Łęgowik, J., & Nowakowska, M. (2011). New bilayer-coated microbead system for controlled release of 5-aminosalicylic acid. *Polymer Bulletin*, *66*(3), 433–443.

Kawadkar, J., Chauhan, M. K., & Ram, A. (2010). Evaluation of potential of Zn-pectinate gel (ZPG) microparticles containing mesalazine for colonic drug delivery. *DARU Journal of Pharmaceutical Sciences*, *18*(3), 211–220.

Lachman, L., Deluca, P., & Akers, M. J. (1987). Kinetic principals and stability testing. In L. Lachman, H. A. Lieberman, & J. L. Kanig (Eds.), *The theory and practice of industrial pharmacy* (pp. 760–803). Bombay: Varghese Publishing House.

Li, Y. Y., Zhang, X. Z., Kim, G. C., Cheng, H., Cheng, S. X., & Zhuo, R. X. (2006). Thermosensitive Y-shaped micelles of poly(oleic acid-Y-N-isopropylacrylamide) for drug delivery. *Small*, *2*(7), 917–923.

Mahato, R. I., & Narang, A. S. (2012). *Pharmaceutical dosage forms and drug delivery* (2nd ed.). United States of America: CRC Press. (biopharmaceutical and physiological considerations).

Palsmeier, R. K., Radzik, D. M., & Lunte, C. E. (1992). Investigation of the degradation mechanism of 5-aminosalicylic acid in aqueous solution. *Pharmaceutical Research*, *9*(7), 933–938.

Pourjavadi, A., Jahromi, P. E., Seidi, F., & Salimi, H. (2010). Synthesis and swelling behavior of acrylatedstarch-g-poly(acrylic acid) and acrylatedstarch-g-poly(acrylamide) hydrogels. *Carbohydrate Polymers*, *79*(4), 933–940.

Prüsse, U., Bilancetti, L., Bučko, M., Bugarski, B., Bukowski, J., Gemeiner, P., et al. (2008). Comparison of different technologies for alginate beads production. *Chemical Papers*, *62*(4), 364–374.

Pushpamalar, V., Langford, S., Ahmad, M., & Lim, Y. (2006). Optimization of reaction conditions for preparing carboxymethyl cellulose from sago waste. *Carbohydrate Polymers*, *64*(2), 312–318.

Pushpamalar, V., Langford, S. J., Ahmad, M., Hashim, K., & Lim, Y. Y. (2013). Preparation of carboxymethyl sago pulp hydrogel from sago waste by electron beam irradiation and swelling behavior in water and various pH media. *Journal of Applied Polymer Science*, *128*(1), 451–459.

Ritger, P. L., & Peppas, N. A. (1987). A simple equation for description of solute release II. Fickian and anomalous release from swellable devices. *Journal of Controlled Release*, *5*(1), 37–42.

Said, H. M., Abd Alla, S. G., & El-Naggar, A. W. M. (2004). Synthesis and characterization of novel gels based on carboxymethyl cellulose/acrylic acid prepared by electron beam irradiation. *Reactive and Functional Polymers*, *61*(3), 397–404.

Saravanan, M., Bhaskar, K., Maharajan, G., & Pillai, K. S. (2004). Ultrasonically controlled release and targeted delivery of diclofenac sodium via gelatin magnetic microspheres. *International Journal of Pharmaceutics*, *283*(1), 71–82.

Schroeder, K. W. (2002). Role of mesalazine in acute and long-term treatment of ulcerative colitis and its complications. *Scandinavian Journal of Gastroenterology*, *37*(236), 42–47.

Tuğcu-Demiröz, F., Acartürk, F., Takka, S., & Konuş-Boyunağa, Ö. (2007). Evaluation of alginate based mesalazine tablets for intestinal drug delivery. *European Journal of Pharmaceutics and Biopharmaceutics*, *67*(2), 491–497.

Vázquez, B., San Roman, J., Peniche, C., & Cohen, M. E. (1997). Polymeric hydrophilic hydrogels with flexible hydrophobic chains. Control of the hydration and interactions with water molecules. *Macromolecules*, *30*(26), 8440–8446.

Vijayabaskar, V., Bhattacharya, S., Tikku, V., & Bhowmick, A. K. (2004). Electron beam initiated modification of acrylic elastomer in presence of polyfunctional monomers. *Radiation Physics and Chemistry*, *71*(5), 1045–1058.

Viseras, M. T., Aguzzi, C., Cerezo, P., Cultrone, G., & Viseras, C. (2009). Supramolecular structure of 5-aminosalycilic acid/halloysite composites. *Journal of Microencapsulation*, *26*(3), 279–286.

Wang, M., Xu, L., Hu, H., Zhai, M., Peng, J., Nho, Y., et al. (2007). Radiation synthesis of PVP/CMC hydrogels as wound dressing. *Nuclear Instruments and Methods in Physics Research Section B: Beam Interactions with Materials and Atoms*, *265*(1), 385–389.

Yang, L., Chu, J. S., & Fix, J. A. (2002). Colon-specific drug delivery: new approaches and in vitro/in vivo evaluation. *International Journal of Pharmaceutics*, *235*(1), 1–15.